ENGINEERING

Super-resolution wearable electrotactile rendering system

Weikang Lin[1,2]†, Dongsheng Zhang[1]†, Wang Wei Lee[1]†, Xuelong Li[1], Ying Hong[2], Qiqi Pan[2], Ruirui Zhang[1], Guoxiang Peng[1], Hong Z. Tan[1]‡, Zhengyou Zhang[1], Lei Wei[1]*, Zhengbao Yang[2]*

The human somatosensory system is capable of extracting features with millimeter-scale spatial resolution and submillisecond temporal precision. Current technologies that can render tactile stimuli with such high definition are neither portable nor easily accessible. Here, we present a wearable electrotactile rendering system that elicits tactile stimuli with both high spatial resolution (76 dots/cm^2) and rapid refresh rates (4 kHz), because of a previously unexplored current-steering super-resolution stimulation technique. For user safety, we present a high-frequency modulation method to reduce the stimulation voltage to as low as 13 V. The utility of our high spatiotemporal tactile rendering system is highlighted in applications such as braille display, virtual reality shopping, and digital virtual experiences. Furthermore, we integrate our setup with tactile sensors to transmit fine tactile features through thick gloves used by firefighters, allowing tiny objects to be localized based on tactile sensing alone.

INTRODUCTION

Technological advances such as the liquid crystal display and organic light-emitting diode display have enabled realistic replication of digitally captured images and videos to our eyes, much like speakers reproducing naturalistic sound recordings to our ears (*1*–*3*). In comparison, a device that can realistically render tactile sensations on our skin is sorely missing. Although researchers have made great progress in developing sensors that digitally capture tactile features with high resolution (*4*, *5*), high sensitivity (*6*, *7*), high temporal precision (*8*), and multiple sensing modalities (*9*), an intuitive stimulation method is needed to effectively virtualize the sense of touch, i.e., the recording and playback of the cutaneous sensation over space and time.

The human somatosensory system shows exquisite spatial and temporal resolution (*10*–*13*). For instance, our fingertips are innervated by high-density mechanoreceptors, allowing us to distinguish spatial features as fine as millimeter precision (*14*, *15*) and encode information with submillisecond precision [0.8 ms for fast-adapting type I (FA-I) afferents] (*16*). An effective tactile feedback system should ideally try to match the fidelity of our tactile perceptual capability in these domains.

Existing techniques to reproduce tactile stimuli can be broadly classified into two categories, mechanical or electrical stimulation. By applying localized mechanical force (*17*, *18*) or vibration (*19*, *20*) on the skin, mechanical actuators can elicit stable and continuous tactile sensations. However, these mechanical actuators tend to be bulky, severely limiting the spatial resolution when integrated into a portable or wearable device. Owing to the mode of actuation, mechanical actuators like linear motors and pneumatic actuators typically suffer from a slow response time (*21*). By comparison, electrotactile stimulators can be light and flexible while offering higher resolution and faster responses (*22*, *23*). However, electrical signals need to be several hundreds of volts to penetrate the high-impedance stratum corneum layer, which poses a safety concern. Moreover, given the high variability in the electrical properties of human skin over time and across individuals, continuous calibration procedures are necessary to ensure that the sensation presented remains within the comfortable range of users (*24*).

To address these limitations, we present a new electrotactile rendering system for displaying various tactile sensations, such as pressure, vibration, and texture roughness in high fidelity. To simulate the natural sense of touch, it is important to understand and mimic the key factors affecting the sensory properties of biological skin. As shown in Fig. 1A, when the skin is deformed by an external force, mechanosensitive ion channels are opened, depolarizing the soma of mechanoreceptors and thus triggering action potentials that are propagated to the somatosensory cortex through peripheral nerve bundles (*25*, *26*). In comparison, our electrotactile device directly generates electrical current at a localized region within the skin, triggering action potentials in the axons of nearby mechanoreceptors, which propagate upstream through the same pathways (*27*, *28*) and are thus interpreted in the brain as tactile stimuli (Fig. 1B). Various sensations can be elicited, including vibration, touch, tingling, itching, and pressure through the variation of the waveform, frequency, duration, or location of the stimulation current (*29*). The electrotactile device consists of an electrode array and a rubber finger cot (Fig. 1C), in which a 5 × 5 fingertip electrode array is fabricated on a piece of a thin flexible printed circuit (FPC) and the contact electrodes are made from 25 half-spherical–shaped metal bumps to maximize the effective contact between the electrode and the irregular surface of the human skin. With a novel high-frequency modulation technique, a much lower stimulation voltage of between 13 and 28 V is sufficient to elicit tactile sensations ranging from a slight touch to a sharp prick. Moreover, we incorporated a closed-loop feedback circuitry that allows our system to quickly respond to changing electrical conditions at the contact electrodes, thus rendering a stable sensation. It is also important to highlight the role of a unique current-steering super-resolution strategy in achieving a high spatial resolution (76 dots/cm^2), which approaches the innervation density of the slowly adapting type I (SA-I) afferents in the fingertip (*30*, *31*). As shown in Fig. 1D, compared to human tactile perception, our electrotactile device shows similar spatial

[1]Robotics X Laboratory, Tencent Technology (Shenzhen) Co. Ltd., Shenzhen, China. [2]Department of Mechanical Engineering, City University of Hong Kong, Hong Kong, China.
*Corresponding author. Email: zb.yang@cityu.edu.hk (Z.Y.); leighwei@tencent.com (L.W.)
†These authors contributed equally to this work as co-first authors.
‡Present address: Purdue University, West Lafayette, IN 47907, USA.

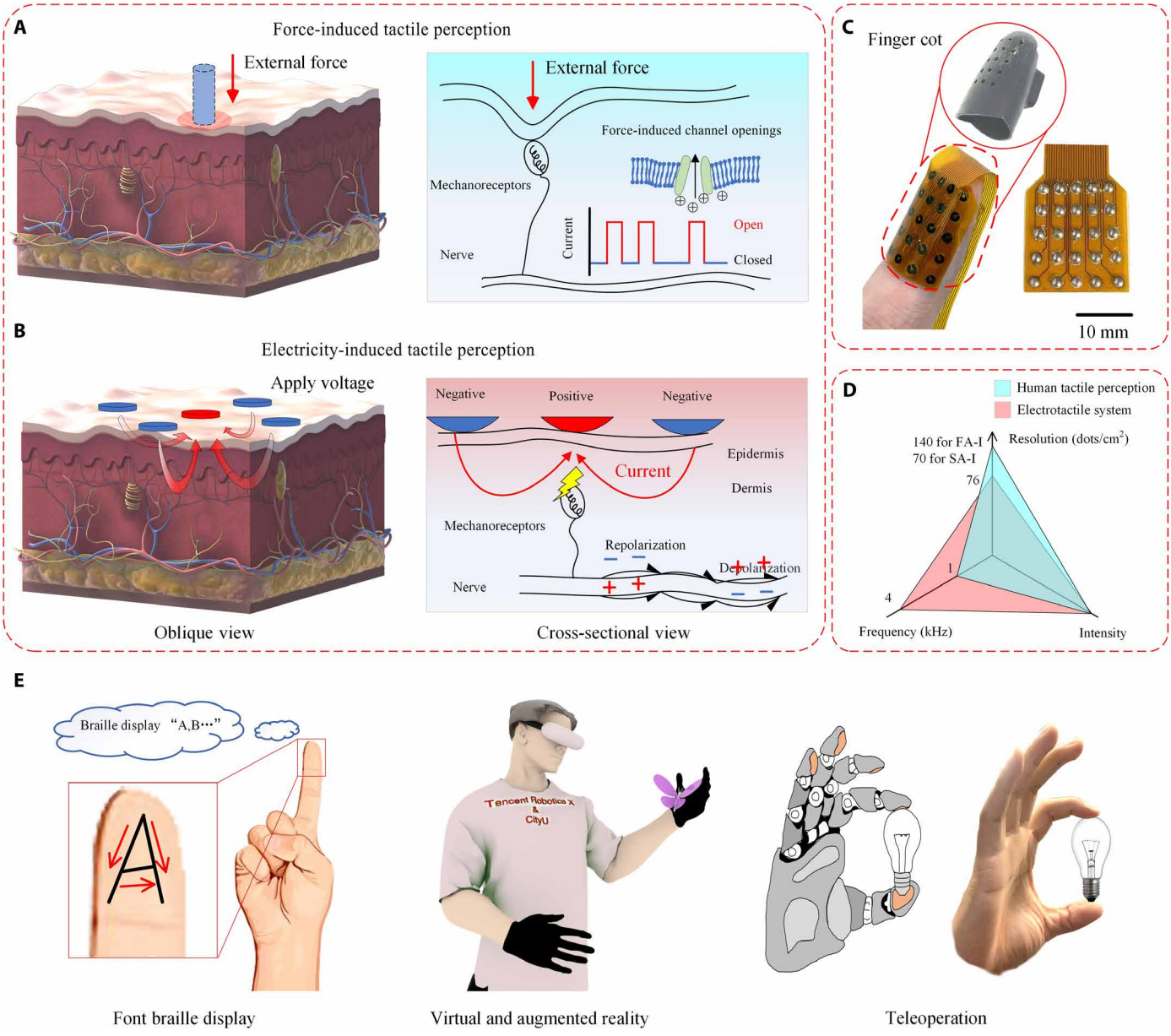

Fig. 1. Design and architecture of the electrotactile rendering system. (**A**) Schematic of the tactile perception of human skins: Strain on the skin induced by an external force triggers the mechanosensitive channels that convert external force into electrochemical and electrical signals. (**B**) Schematic of the electrotactile system whereby current is induced in the skin to stimulate mechanoreceptors and nerves, generating action potentials that are interpreted as tactile signals by the brain. (**C**) Optical images of the electrotactile device, an FPC with 25 half-sphere electrodes attached in a rubber finger cot. (**D**) Comparison between human tactile perception and the electrotactile rendering device in spatial resolution, refresh rates, and intensity range. (**E**) Demonstrations of the electrotactile system in braille display, VR and augmented reality, and teleoperation.

resolution and much higher refresh rates and covers the full human tactile intensity range.

The effectiveness of our electrotactile rendering system is evaluated through a user study whereby 20 volunteers were tasked to identify tactile sensations such as intensity, roughness, texture, and other complex patterns. The ability to evoke tactile sensations with unprecedentedly fine control over its location and duration opens up unique opportunities in rendering methods. Specifically, we exploit the tactile continuity illusion (*32*) to render numbers and letters as spatiotemporally distinct strokes that mimic the order in which they are written. This approach, which we define as font braille, allows the visually impaired to use the same system to read and write as a normal person would. We also highlight the applicability of our technology to virtual reality (VR) shopping of clothes as well as digital virtual experience. Last, we integrate our electrotactile rendering system with tactile sensors on a thick glove, enhancing the tactile acuity of the wearer and allowing him to locate a tiny object, which would otherwise be impossible because of the mechanical insulation of the gloves. We envision that our technology will benefit a broad spectrum of applications such as information transmission, surgical training, teleoperation, and multimedia entertainment (Fig. 1E).

RESULTS

Low-voltage tactile stimulation through dual high-frequency alternating current modulation

Unlike most electrotactile stimulators that rely on high-voltage direct current (DC) pulses to penetrate the high-impedance stratum corneum layer (*22*, *33*), we adopt a high-frequency alternating current (AC) to overcome the insulation. As shown in Fig. 2A, the electrical impedance at every layer of the human skin can be modeled as a resistor and capacitor in parallel. Hence, high-frequency AC can penetrate the human skin and stimulate nerves. To theoretically investigate the relationship between skin impedance and stimulating current frequency, a finite element analysis (FEA) simulation based on COMSOL Multiphysics is carried out using parameters (*34*–*37*) defined in table S1. As shown in Fig. 2B, increasing the frequency of the AC stimulation results in higher current density and deeper skin penetration, translating to the activation of more nerves and

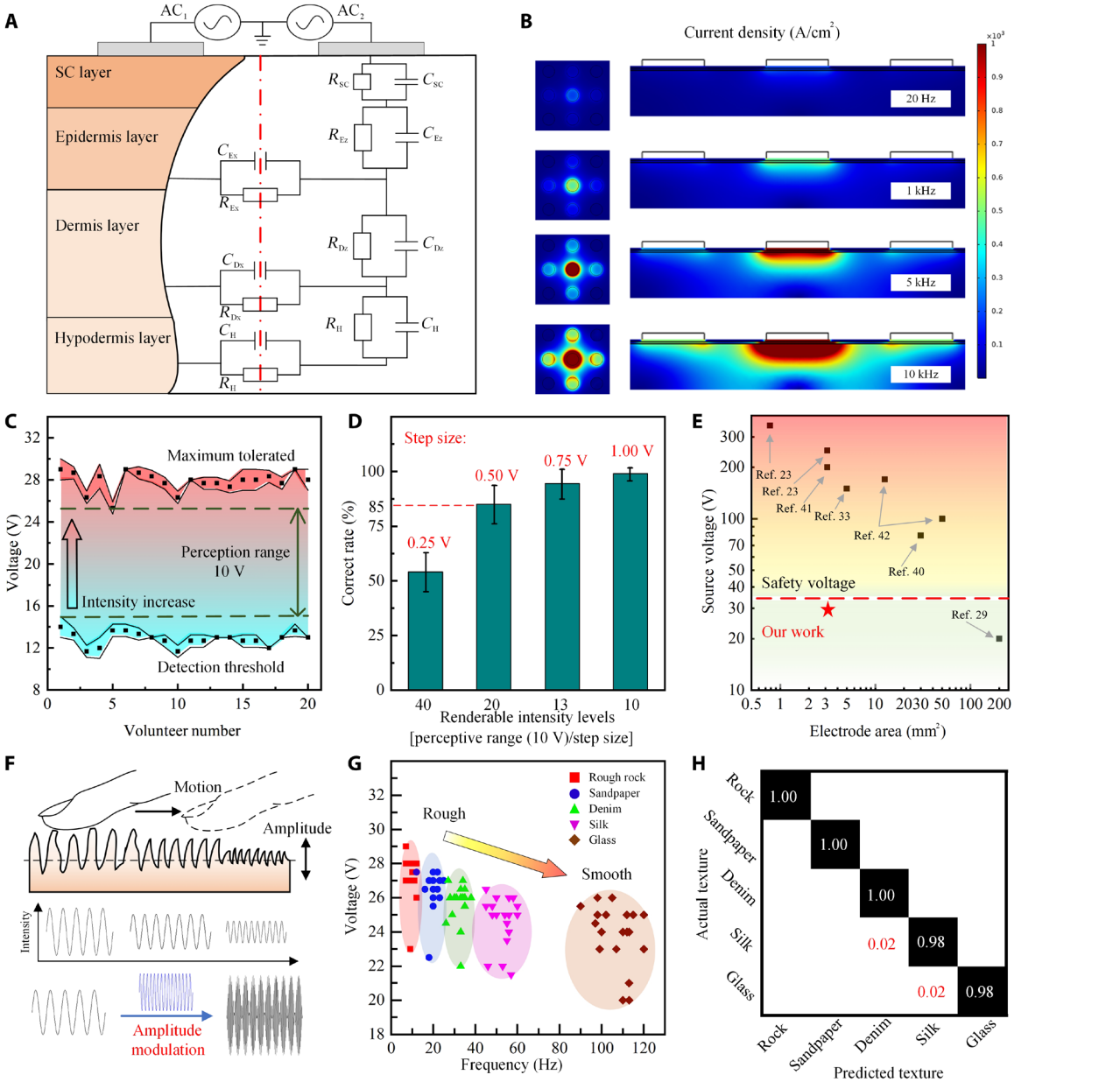

Fig. 2. The simulation and experimental results of electrical stimulation using high-frequency AC. (**A**) Schematic illustration of electrical impedance model and equivalent circuit of the human skin. SC, stratum corneum. (**B**) Simulation results of current density distribution at different frequencies. (**C**) Relationship between tactile perception intensity and stimulation voltage; as the voltage increases, the intensity gradually increases from a slight touch to a sharp prick. Error bars indicate the fluctuation of the test results of each volunteer in multiple measurements. (**D**) Ability of the electrotactile system to render different tactile intensities. The number of renderable intensity levels can be changed by adjusting the step size of each changed voltage. Users can feel 20 different intensity levels with 85% accuracy. Error bars show the SD between 20 volunteers. (**E**) Comparison of the applied voltage and electrode areas in this work with other electrotactile devices. (**F**) Illustration of the roughness perception, which is mainly determined by intensity and vibration frequency. (**G**) Relationship between the roughness perception and stimulation voltage and frequency. (**H**) Classification confusion matrix of five different roughness surfaces.

thus rendering a stronger tactile sensation. As the frequency of stimulating current increases from 20 to 10 kHz, the fingertip skin impedance decreases is notable, which agrees with the experimental results (fig. S1). The tactile perception is further intensified by stimulation with two AC currents of the same parameters but with 180° phase difference. Using our dual high-frequency AC strategy, tests on volunteers show that a stimulation voltage between 13 V (detection threshold voltage) and 28 V (maximum tolerated voltage) is sufficient to elicit tactile sensations ranging from a slight touch to a sharp prick (Fig. 2C).

While the stimulation voltage can be controlled with millivolt precision, it is important to determine the minimum perceptible voltage difference under our stimulation paradigm as it translates to the level of variability of the rendered sensation. The comfortable perceptive range is from about 15 to 25 V (Fig. 2C), and we define the renderable intensity levels as the perceptive range (10 V) divided by step size (0.25, 0.5, 0.75, and 1 V). As shown in Fig. 2D, with the increase of tactile intensity levels, the intensity discrimination accuracy decreases accordingly. On the basis of the results, variation of the stimulation voltage into steps of 0.5 V is perceivable for 85% of the subjects, which corresponds to at least 20 uniquely distinguishable intensity levels. This is much higher than earlier works (4, 3, and 2 intensity levels, respectively) (*18*, *38*, *39*).

Another challenge of electrotactile rendering is the inverse relationship between electrode size and stimulation voltage. Smaller electrode sizes are needed to achieve a higher spatial resolution, which, in turn, leads to increased contact impedances that require dangerously high voltages to overcome. Figure 2E compares recent electrotactile stimulators (*22*, *23*, *29*, *33*, *40*–*42*) in terms of applied voltage and electrode size. Our dual high-frequency AC strategy enables a spatial resolution of 25 dots per fingertip with a maximum applied voltage of 30 V, thus simultaneously achieving a high resolution while eliminating safety concerns.

Amplitude modulation for roughness perception rendering

Roughness perception is mainly determined by the tactile intensity and vibration frequency, where the presence of high-intensity, low-frequency tactile signals is often associated with rough surfaces (Fig. 2F). Our stimulation technique achieves the same effect by using amplitude modulation (AM). Essentially, a high-frequency (10 kHz) square carrier wave is used to modulate the lower-frequency sine-waved vibration signal. To study the efficacy of AM on roughness perception, we invited volunteers to adjust the amplitude and frequency of the lower-frequency signal to approximate the sensation felt when touching five surfaces of different roughness, namely, rough rocks, sandpaper (60 grit), denim, silk, and glass (fig. S2). Volunteers wore the electrotactile device on their left index finger and used their right index finger to physically touch the five surfaces. The results (Fig. 2G) indicate that low-frequency and high-voltage stimulation best simulates rough textures like rocks and sandpaper, while high-frequency and low-voltage stimulation renders smooth textures such as silk and glass, which is consistent with the natural human tactile perception (*43*). Note that the volunteers show an extremely high level of recognition accuracy (98%) of the different roughness rendered by the electrotactile system (Fig. 2H).

Electrotactile control system

The main components of our system are described in Fig. 3A, and a full picture of electrotactile devices is shown in fig. S3. A microcontroller unit (MCU) controls the multichannel digital-to-analog converter (DAC) chip to generate two high-frequency waveforms (fig. S4). These waveforms are then amplified to the desired stimulation voltages AC_1 and AC_2 (Fig. 3B). A current monitoring circuit is used to detect changes in contact impedance, which may occur due to sweating or changes in the skin contact area. A calibration procedure is performed, where five electrodes are sequentially connected to AC_1 for 100 ms, corresponding to a left-to-right movement of the stimulated region on the fingertip. Adjustments are then made to subsequent stimulation voltages to ensure a consistent stimulation current (Fig. 3C). Last, a switch array is used to determine the state of the electrodes (fig. S5), where each electrode may be connected to AC_1 or AC_2 or left floating. The switches can be dynamically reconfigured at a frequency of as high as 4 kHz (fig. S6), allowing the stimulation pattern to be rendered with submillisecond precision. Last, a computer working as the terminal of the human-machine interface communicates and controls all the aforementioned components to form a holistic close-looped electrotactile rendering system (*44*).

Super-resolution stimulation through current steering

While having 25 electrodes per fingertip may be state of the art, the fingertip is capable of resolving touch with far higher spatial acuity. We capitalize on the high reconfigurability of our electrode array to perform stimulation at locations in between physical electrodes, thus achieving super-resolution (Fig. 4A). For instance, stimulation of sites directly under a physical electrode is considered a normal resolution site. Stimulation of a normal resolution site is accomplished by connecting the target electrode to AC_1 and the four surrounding electrodes to AC_2. By creating asymmetry in the distribution of AC_2-connected electrodes around the AC_1-connected electrode, the stimulation current is skewed toward the region with more AC_2 electrodes. As the resultant stimulation site under this current steering technique is between two physical electrodes, we define it as a super-resolution site. FEA simulations show that the degree of skew can be controlled by the level of asymmetry (Fig. 4B). Our present prototype with 25 electrodes allows for two super-resolution sites between every pair of electrodes for the 9 central electrodes, and one super-resolution site per electrode pair at the edges. The total number of discrete stimulation sites thus increases from 9 to 49 for the central region and from 25 to 105 for the entire fingertip (Fig. 4C). Notably, the effective tactile spatial resolution in the center area is as high as $49/(0.8 \times 0.8) = 76$ dots/cm^2, which is similar to the density of SA-I mechanoreceptors in the human skin. Detailed electrode configurations to stimulate each super-resolution site are described in fig. S7. Our current steering super-resolution strategy thus increases the spatial resolution with no extra hardware.

We evaluate the tactile perception of super-resolution sites, and the result shows that there is no obvious difference between normal resolution sites in the intensity test (fig. S8). In addition, the volunteer can clearly recognize (96% accuracy) the spatial position of super-resolution sites (fig. S9). To further assess the efficacy of current steering in physical experiments, volunteers are tasked to distinguish patterns including curves with slightly different angles and ellipses with small changes in aspect ratios (Fig. 4D). Differences between the patterns are very small and can only be rendered using super-resolution. The results demonstrate the effectiveness of our current steering approach, where the recognition accuracy of curves and ellipses is 84 and 90%, respectively.

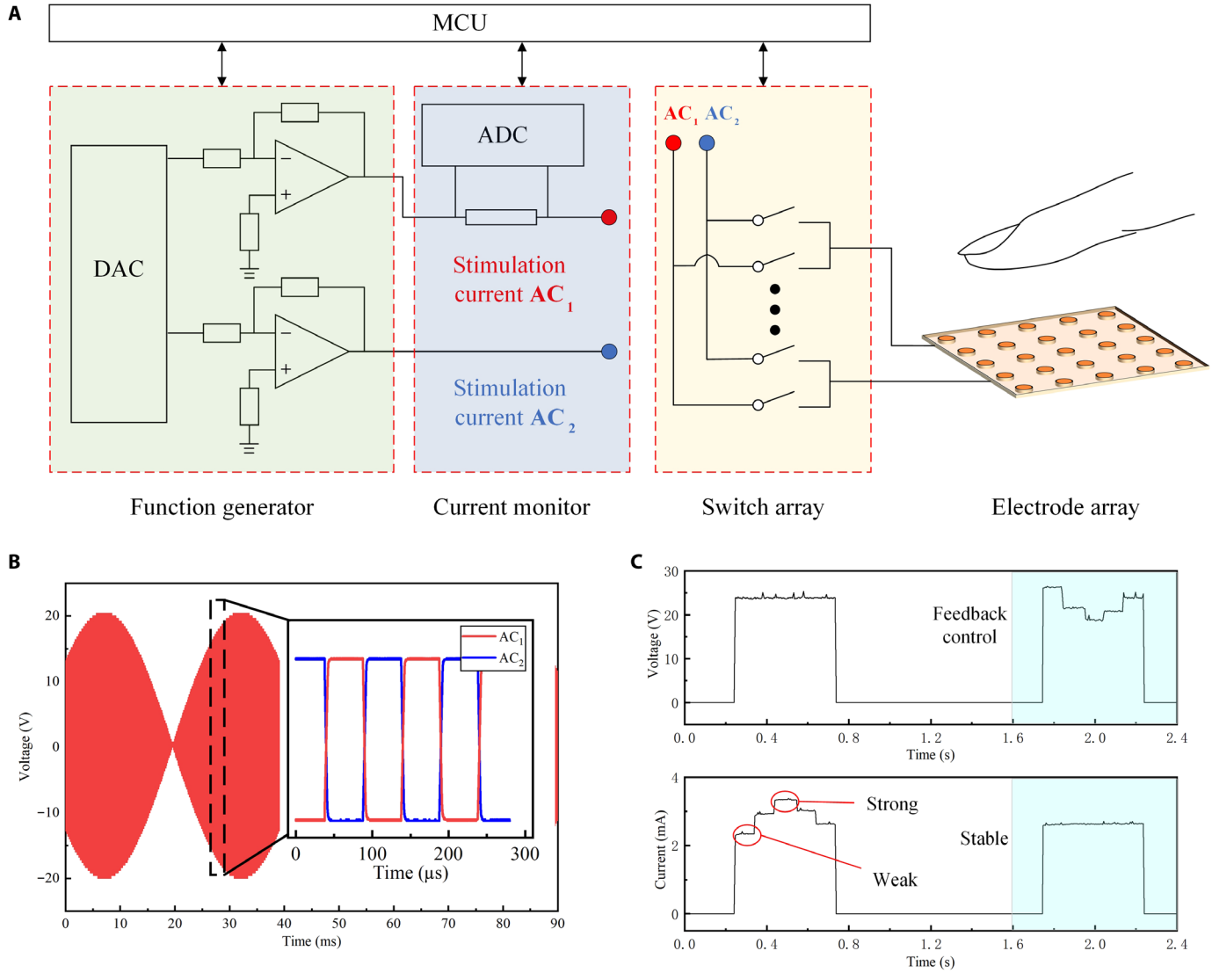

Fig. 3. The structure of the electrotactile rendering system. (**A**) Schematic diagram of the control system, which consists of three parts. Function generator generates the desired stimulation current AC_1 and AC_2, current monitor ensures the consistency of output perception by feedback control, and switch array manages the state of each electrode separately. ADC, analog-to-digital converter. (**B**) Waveform of the stimulation current. Ten kilohertz of square wave is amplitude-modulated by 40-Hz sine wave. (**C**) Stable electrotactile perception under the feedback control strategy, where the stimulation voltage is changed according to the measured current.

A spatiotemporal approach to text rendering

One major problem faced by the visually impaired when learning braille is the disconnect between the systems used for reading and writing (*45*). Leveraging the ability to evoke tactile sensations with ultrafine spatiotemporal control, we propose a tactile reading system that consists of numbers and letters rendered as spatiotemporally discrete strokes that mimic the order in which they are written. This approach, which we define as font braille, makes use of the tactile continuity illusion whereby sensory inputs distinct in space and time are naturally pieced together by our somatosensory system to form a continuous sensation (*46*). Using font braille, the visually impaired would be able to use the same alphabetical system to read and write.

Font braille consists of two major parts, namely, the code and the rendering sequence. We break down the letters of the alphabet as well as numerical digits into individual strokes and order them the way in which they are written (Fig. 5A). We take advantage of the fact that tactile perception is more sensitive to dynamic features such as the start, end, and sequence in which the stroke is drawn, instead of the absolute location where the stroke is rendered. Font braille can thus be simplified to consist of only 16 basic strokes (Fig. 5B) that span the entire electrode array. The combination and sequence of these basic strokes can effectively represent almost all numbers and alphabets except for the letter "O" and the number "0," which needs to be rendered by including super-resolution sites. Tests with volunteers show a recognition accuracy of over 87% (Fig. 5C). Analysis of the confusion matrix shows that the most easily confused characters are "I" and "1," "S" and "8," and "O" and "0" (detailed confusion matrix is shown in fig. S10). Recognition accuracy can be further improved by optimizing stimulation parameters (such as the relative location, intensity, and duration of strokes) according to personal preferences. Figure 5D illustrates the use of

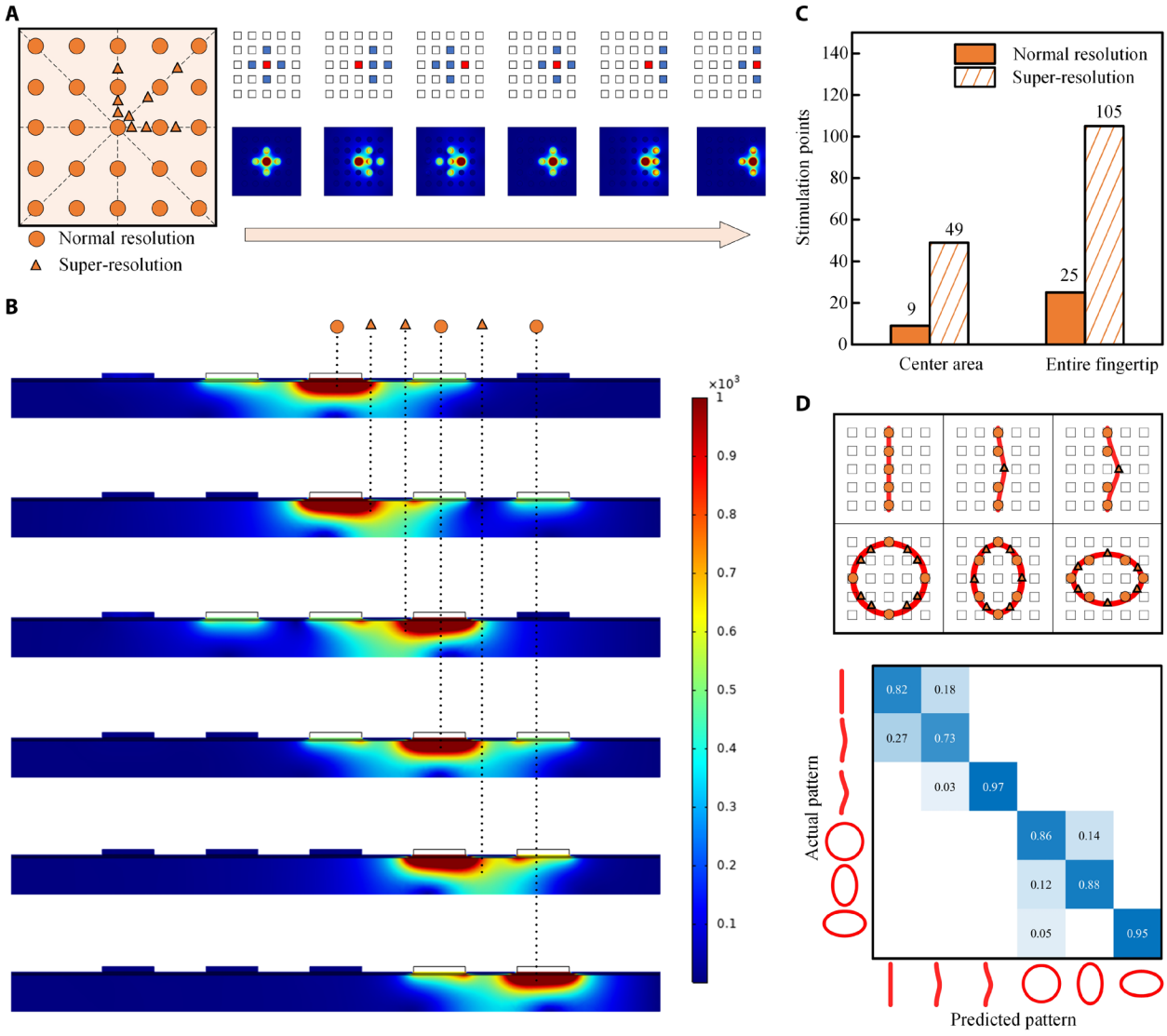

Fig. 4. Beam-forming super-resolution control strategy. (**A**) Illustration of the 5 × 5 electrotactile device rendering resolution (left) and the top view of simulation results of current density under the different distribution of stimulation electrodes (right). The 25 squares represent the actual distribution of electrodes, in which the red, blue, and blank represent the states of the electrodes in AC_1, AC_2, and floating, respectively. (**B**) Cross-sectional view of simulation results of current density under the different distribution of stimulation electrodes. (**C**) Improvement of tactile rendering resolution under the super-resolution strategy. (**D**) Schematic of different patterns of rendering strategy and these patterns' recognition confusion matrix, where the circle dot means normal resolution site and the triangle dot is super-resolution site.

font braille in a practical setting, where a volunteer deciphers the character rendered by the fingertip electrotactile device and writes it down (movie S1).

VR and sensor-actuator glove system

Besides being a tool for the visually impaired, our electrotactile stimulation technique is well suited for VR applications. For instance, the high spatiotemporal control of haptic stimulation is particularly well suited for rendering the texture of clothes in a virtual shopping scenario (Fig. 6A). The electrodes can also be made highly flexible and scalable to cover larger areas such as the palm (fig. S11). Working together with the fingertip electrodes, we demonstrate a VR cat interaction session where the user experiences the itchy sensation in the fingertips when licked by a cat's tongue that is covered by hard barbs (Fig. 6B). Moreover, when stroking the cat's fur, variances in roughness can be conveyed to the palm as the stroking changes in direction and speed (movie S2).

Another interesting application is the transmission of fine tactile details through thick gloves. We integrate the thin and light electrodes of our electrotactile rendering system together with flexible tactile sensors on a safety glove (Fig. 6C). The tactile sensor array captures the pressure distribution on the exterior of the glove and relays the information to the user in real time through tactile stimulation. Figure 6D demonstrates the scenario where the volunteer quickly and accurately locates a tiny steel washer (1 mm radius and 0.44 mm thick) using only tactile feedback from the sensorized glove (movie S3 and fig. S12). The task represents the restoration of high-fidelity tactile perception that is currently unavailable to astronauts, firefighters, and deep-sea divers because of insulation from their protective suits.

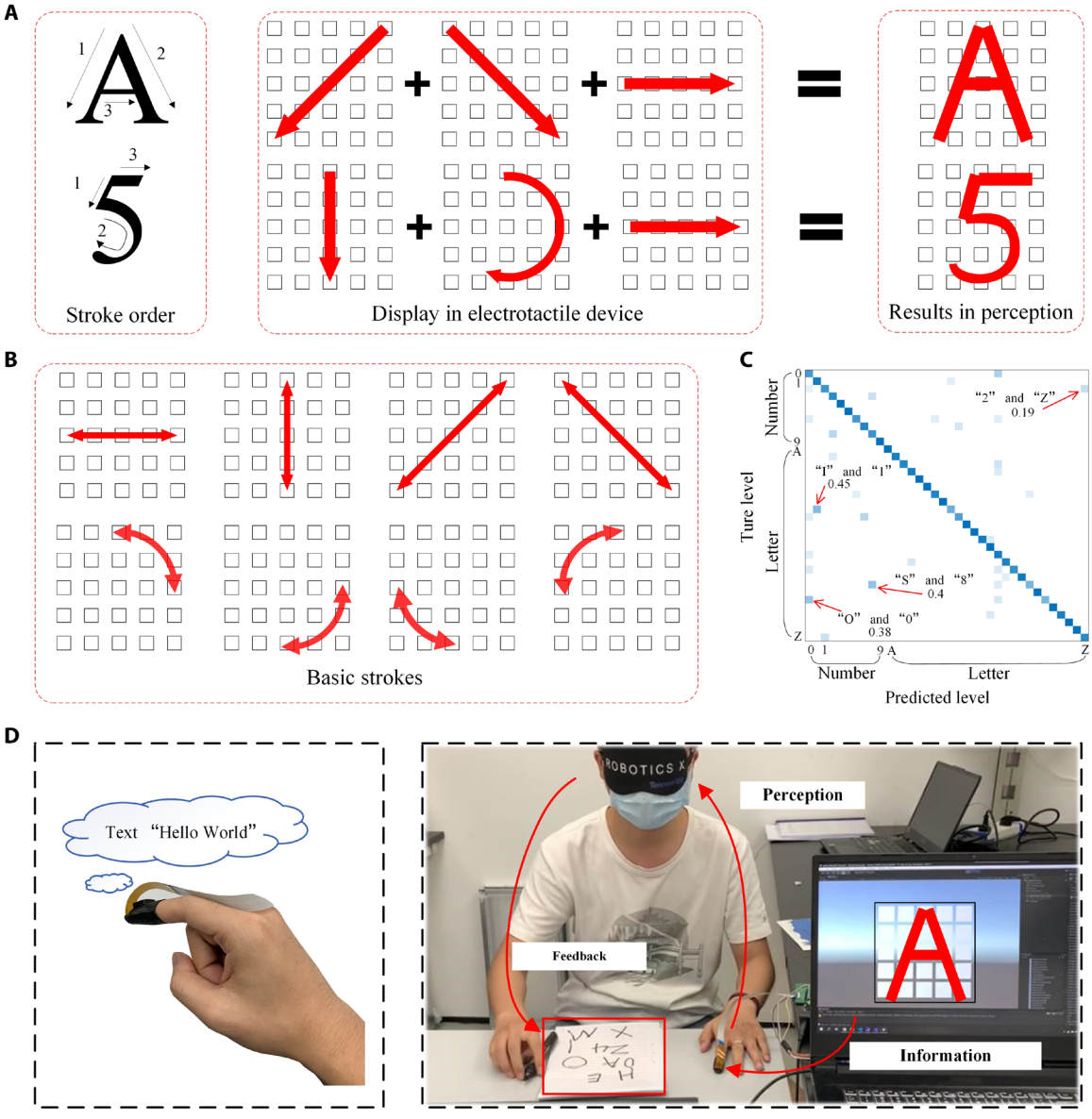

Fig. 5. Font braille strategy for letters and numbers display. (**A**) Stroke order of alphabet "A" and number "5" and its control strategy of the tactile rendering based on the font braille strategy. (**B**) Sixteen kinds of basic stroke order in the font braille strategy. (**C**) Confusion matrix of the English alphabet and numbers. Some among them would still be confused such as "I" and "1," "S" and "8," "O" and "0," and "2" and "Z". (**D**) Schematic (left) and demonstration (right) of text information transmission through the electrotactile device.

DISCUSSION

The electrotactile rendering system introduced here is unique on several fronts. Compared to mechanical-based stimulators such as the pneumatically actuated HaptX gloves or vibration-based haptic skin (*20*), our system is flexible, thin, and light and can thus be integrated with existing clothing such as gloves or expanded to cover more areas such as the palm without being excessively bulky. Our system also demonstrated unique advantages in tactile rendering performance, such as a wider gamut of perceivable tactile sensations, ultrafast refresh rate, and superior spatial resolution. In comparison to other electrical stimulators, our dual high-frequency AM-modulated signal simultaneously achieves high spatial resolution and low-voltage stimulation. Notably, the tactile sensation can be elicited at voltages an order of magnitude lower than existing systems without the need for invasive interfaces such as microneedles (*47*). At the same time, the electrodes used are small—25 electrodes were fitted onto a fingertip-sized stimulator array. Combined with current steering techniques, stimulation can be performed with super-resolution of up to 76 dots/cm^2, approaching the density of SA-I mechanoreceptors in the fingertip. Moreover, our system incorporates closed-loop feedback circuitry that dynamically compensates for the variations in skin contact conditions of individual electrodes, ensuring a stable and comfortable tactile rending performance.

A common weakness of all electrical-based stimulators is the inability to precisely stimulate just the SA mechanoreceptors without activating the FA receptors, making it difficult to produce the

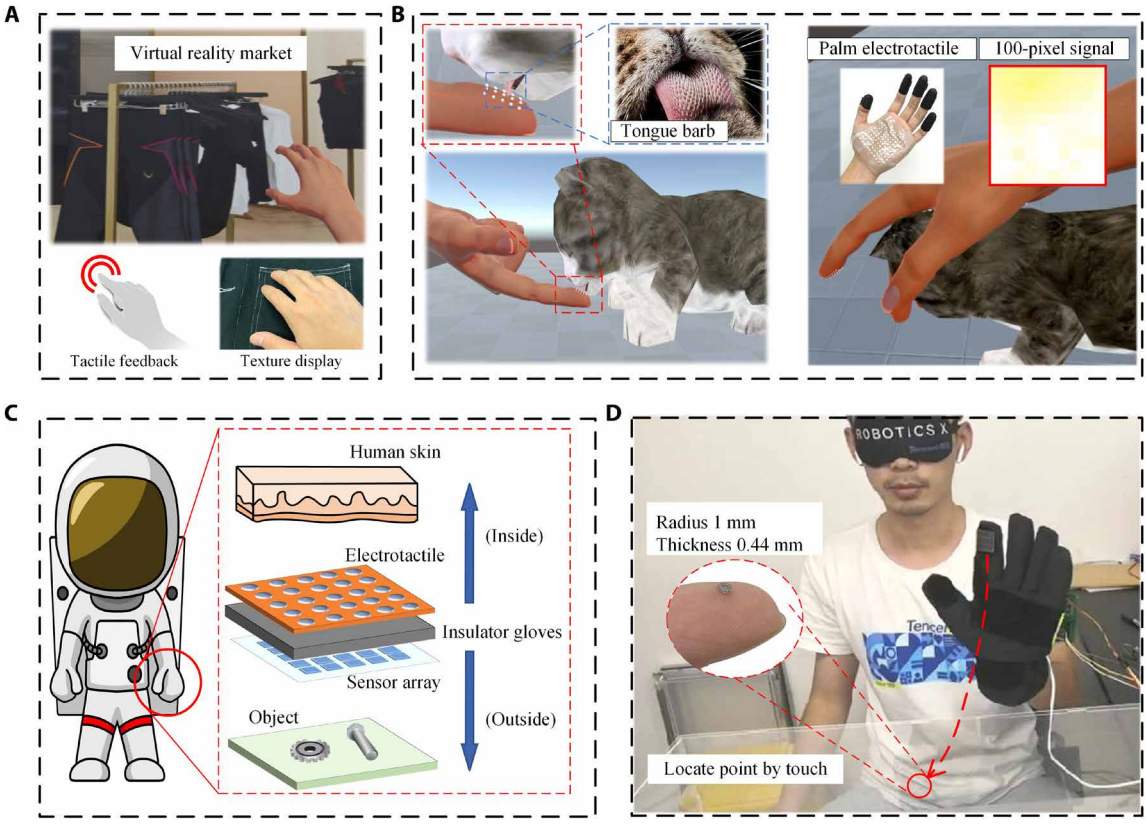

Fig. 6. Applications of the electrotactile rendering system. (**A** and **B**) Examples of the electrotactile in virtual and augmented reality. (A) Feeling the touch and texture of clothes in VR shopping. (B) Touch communication with a virtual cat to feel a sense of itchy in the finger and enjoy the touch feeling of petting cat through the palm electrotactile device. (**C**) Illustration of tactile restoring for astronauts carrying out crucial tasks. The sensor array is attached outside of the glove to sense the object, and the electrotactile device is attached inside to render the tactile information. (**D**) Demonstration of fast and precise positioning of a tiny part while wearing a thick protective glove by electrotactile rendering system.

sensation of sustained pressure. While some research speculated on the possibility of stimulating specific types of afferents by changing the polarity of the electrodes (*48*), there is currently no work that verifies this capability in a conclusive manner. Nevertheless, the dynamic nature of touch meant that the response of FA receptors plays a dominant role in facilitating rapid tactile perception (*30*). Thus, coupled with suitable stimulation patterns, the ability to precisely activate the receptors in time and space may provide sufficient feedback for users to accomplish functional tasks, even if the sensation lacks the realism that a physical interaction provides. Moreover, given that the electrodes are very flexible and lightweight, they can be combined with other haptic feedback modalities if greater authenticity is desired.

Having a tactile rendering system with high spatiotemporal resolution opens up unique possibilities. We took advantage of the tactile continuity illusion to render numbers and letters in a fashion similar to which they are written, providing the visually impaired with a consistent representation when reading and writing. Our system is also well suited for VR applications such as online shopping or haptic interaction with virtual objects. Last, a sensor-actuator system was demonstrated to bring back fine tactile sensations to wearers of thick protective gloves. To the best of our knowledge, our tactile restitution glove system is the first of its kind that successfully enables the accurate localization of tiny components through tactile perception alone. All these demonstrations convey the wide-ranging applicability of the electrotactile system and outline a promising route toward future information transmission, entertainment, education, training, and teleoperation.

MATERIALS AND METHODS

Fabrication of the fingertip electrotactile device

The 5 × 5 fingertip electrode array is a piece of thin FPC with 25 copper pads. Additional solder was added to the pads to form half-spherical contact electrodes. Subsequently, the silver film was sputtered on the solder surface to ensure the biocompatibility of the electrotactile device. The electrode radius is about 1 mm, and the center-to-center distance between two adjacent electrodes is approximately 4 mm. The distance gradually decreases from the first knuckle to the tip of the fingertip, according to the structure of the human fingertip. Such a distribution of the electrode array and the half-spherical shape ensure close contact with the human skin. The flexible circuit is fixed in a rubber finger cot by very high bonding tape. The rubber finger cot is then connected to other wearable devices such as protective gloves or exoskeletons.

Fabrication of the stretchable palm electrotactile device

The 10 × 10 electrode array fabricated by screen printing technology shows the potential of large-area electrotactile device fabrication in a low-cost method. The radius of each electrode is 1.5 mm, and

the distance between two adjacent electrodes is 6 mm. We use the stretchable silver paste (DuPont, ME602) as the conductor material and stretchable thermoplastic polyurethane film (110 μm; Shanghai Xin Gen Eco-Technologies) as the substrate. The design pattern was fabricated on a 200 threads per inch polymer mesh and printed using a semiautomated press (Bojing Printing Equipment Co., China; BJ-3050). Sintering of the silver paste was performed at 120°C in a box oven for 20 min. An additional thermoplastic polyurethane (TPU) film (20 μm thickness) with openings for the electrodes was laminated onto the circuit to insulate the connectors from the skin. As shown in fig. S11, the stretchable electrode device still works when stretched under 30% strains or undergoing 500 stretching cycles under 10% strain.

Fabrication of the tactile sensor array

A 6 × 6 tactile sensor array was fabricated on the FPC, while the transducers were made from carbon impregnated polymer (Velostat, 3M). A readout circuit is adapted from Shu *et al.* (*49*). Note that, as the array was initially designed for an earlier project and subsequently repurposed for this demonstration, the data from the sixth row and column were not used for haptic rendering.

Control system

The MCU (STM32F103CBU6) controls the DAC chip (LTC2666) to generate stimulation current waveform through serial peripheral interface (SPI) communication. To make sure that the phase between the two stimulation current waveforms is 180°, the data of the first channel are written into the input register for temporary storage until the data of the second channel are transmitted. Then, the data of the two channels are synchronously updated to the DAC register for the waveform output. The frequency of the resulting square waves can be adjusted from 1 Hz to 100 kHz in a user-definable way through the software interface. The program incorporated an interrupt mechanism to ensure the same interval time of each instruction by timer update interrupt (100-kHz interrupt frequency). The information about voltage amplitude, frequency, and the waveform is sent through direct memory access (DMA)–SPI. Hence, it not only ensures the accuracy of the signal cycle but also updates the signals in time.

The specific waveform signals generated by the signal generator are amplified by the power amplifier (FPA1016, FEELTECH Technology Co. Ltd.) as the input signal of the switch circuit board. Each stimulation electrode is controlled independently through the switch chip (MAX14757). To prevent the short-circuit condition between AC_1 and AC_2, the statement of the electrode is set to high impedance before changing to its opposite state.

An analog-to-digital converter chip (ADS131E08, 64-kSPS sample rate) is used to measure the circuit current for feedback control. The collected data are processed by an averaging filtering algorithm to obtain the envelope of the current amplitude. When the program starts, each electrode applies a small voltage and the amplitude of the current at each point is recorded for the controller.

Experiments with human subjects

The experiments with human subjects were performed in compliance with all the ethical regulations under a protocol that was approved by the City University of Hong Kong Research Committee (application no. H002852). Twenty volunteers participated in this experiment. All of the volunteers gave written informed consent about the experimental procedure. All participants were trained to manipulate the electrotactile system with the help of experimenters until they understood the sensation of electrical stimulation. Participants were asked to clean their fingers with alcohol and apply a thin film of conductive paste (Weaver, Ten20) at the start of the session. To minimize the effect of sensory adaptation, participants were given a 10-min break between trials. For all recognition tests, volunteers underwent a 5- to 10-min familiarization phase to acclimatize themselves with the task. A 10-kHz square wave was used as the carrier wave for all trials. The detailed experimental procedures for each experiment are outlined below.

Experiment 1: Tactile perception at different voltage amplitudes

To test the relationship between the perceived tactile intensity and the voltage amplitude, the stimulation signal consisted of an AM-modulated 40-Hz sine wave that lasted 400 ms, followed by 1000 ms of silence. The amplitude of the modulated wave was gradually increased until the subject reported a noticeable sensation. The reading was recorded as the threshold voltage. The voltage was subsequently increased until the volunteer started to feel uncomfortable, and the reading was regarded as the maximum tolerated voltage amplitude. The process was repeated three times for each subject.

Experiment 2: Minimum perceptible change in tactile intensity

The test began by delivering a signal between 15 and 25 V, which was determined in experiment 1 to be the comfortable range for all subjects. A slight change in the voltage (0.25, 0.5, 0.75, and 1 V) was then made, and the volunteer was asked if a difference could be perceived. The process was repeated 20 times for each volunteer.

Experiment 3: Roughness matching with stimulation voltage and frequency

In this test, volunteers wore the electrotactile device on their left index finger and touched different texture samples with their right index finger. The samples include rough rocks, 60-grit sandpaper, denim, silk, and glass. Volunteers were tasked to adjust the voltage amplitude and frequency of the AM stimulation wave to match the tactile sensation felt by the index fingers on both hands. Each volunteer was tested three times, and the voltage amplitude and frequency were recorded to form a texture dataset for subsequent experiments.

Experiment 4: Rendering surface textures with different roughness

On the basis of the information collected in experiment 3, the stimulation profile (voltage amplitude and frequency of AM signal) for a particular texture was presented to the volunteer in random order. The volunteer was then asked to identify the texture. The process was repeated 20 times for each volunteer.

Experiment 5: Distinguishing spatial position of super-resolution sites

The center normal resolution site and four surrounding super-resolution sites (see fig. S9) were randomly selected and displayed on the fingertip of volunteers. The volunteer was then asked to identify the position. The process was repeated 10 times for each volunteer.

Experiment 6: Distinguishing patterns rendered with current steering

Six special designated patterns (see Fig. 4D) were randomly selected and displayed on the fingertip of volunteers. The volunteer was then asked to identify the pattern. The process was repeated 10 times for each volunteer.

Experiment 7: Character recognition using font braille

The experiment began by rendering a randomly selected alphabet or digit as strokes, where each stroke consisted of a specific sequence of stimulation over several sites. The amplitude of the stimulation current was 20 V, and the frequency was 60 Hz. Stimulation for each site lasted at least 75 ms, and a gap of 500 ms was placed between the end of a stroke and the beginning of the next stroke. The subject was asked to identify the character after all strokes were rendered. Each volunteer was tested 10 times.

SUPPLEMENTARY MATERIALS

Supplementary material for this article is available at https://science.org/doi/10.1126/sciadv.abp8738

REFERENCES AND NOTES

1. H. W. Chen, J. H. Lee, B. Y. Lin, S. Chen, S. T. Wu, Liquid crystal display and organic light-emitting diode display: Present status and future perspectives. *Light Sci. Appl.* **7**, 17168 (2018).
2. Y. Huang, E. L. Hsiang, M. Y. Deng, S. T. Wu, Mini-LED, micro-LED and OLED displays: Present status and future perspectives. *Light Sci. Appl.* **9**, 105 (2020).
3. J. Zhu, X. Liu, Q. Shi, T. He, Z. Sun, X. Guo, W. Liu, O. B. Sulaiman, B. Dong, C. Lee, Development trends and perspectives of future sensors and MEMS/NEMS. *Micromachines* **11**, 7 (2020).
4. W. W. Lee, Y. J. Tan, H. Yao, S. Li, H. H. See, M. Hon, K. A. Ng, B. Xiong, J. S. Ho, B. C. K. Tee, A neuro-inspired artificial peripheral nervous system for scalable electronic skins. *Sci. Robot.* **4**, eaax2198 (2019).
5. S. Sundaram, P. Kellnhofer, Y. Li, J. Y. Zhu, A. Torralba, W. Matusik, Learning the signatures of the human grasp using a scalable tactile glove. *Nature* **569**, 698–702 (2019).
6. H. Yao, W. Yang, W. Cheng, Y. J. Tan, H. H. See, S. Li, H. P. A. Ali, B. Z. H. Lim, Z. Liu, B. C. K. Tee, Near-hysteresis-free soft tactile electronic skins for wearables and reliable machine learning. *Proc. Natl. Acad. Sci. U.S.A.* **117**, 25352–25359 (2020).
7. N. Bai, L. Wang, Q. Wang, J. Deng, Y. Wang, P. Lu, J. Huang, G. Li, Y. Zhang, J. Yang, K. Xie, X. Zhao, C. F. Guo, Graded intrafillable architecture-based iontronic pressure sensor with ultra-broad-range high sensitivity. *Nat. Commun.* **11**, 209 (2020).
8. W. W. Lee, S. L. Kukreja, N. V. Thakor, Live demonstration: A kilohertz kilotaxel tactile sensor array for investigating spatiotemporal features in neuromorphic touch, in *Proceedings of the IEEE Biomedical Circuits and Systems Conference: Engineering for Healthy Minds and Able Bodies (BioCAS 2015)* (IEEE, 2015), pp. 1–4.
9. W. Lin, B. Wang, G. Peng, Y. Shan, H. Hu, Z. Yang, Skin-inspired piezoelectric tactile sensor array with crosstalk-free row+column electrodes for spatiotemporally distinguishing diverse stimuli. *Adv. Sci.* **8**, 2002817 (2021).
10. A. I. Weber, H. P. Saal, J. D. Lieber, J.-W. Cheng, L. R. Manfredi, J. F. Dammann III, S. J. Bensmaia, Spatial and temporal codes mediate the tactile perception of natural textures. *Proc. Natl. Acad. Sci. U.S.A.* **110**, 17107–17112 (2013).
11. B. Pleger, A. Villringer, The human somatosensory system: From perception to decision making. *Prog. Neurobiol.* **103**, 76–97 (2013).
12. E. L. Mackevicius, M. D. Best, H. P. Saal, S. J. Bensmaia, Millisecond precision spike timing shapes tactile perception. *J. Neurosci.* **32**, 15309–15317 (2012).
13. R. T. Verrillo, G. A. Gescheider, Perception via the sense of touch. *Tactile Aids Hear. Impair.*, 1–36 (1992).
14. M. M. D. Cellis, R. M. D. Pool, Two-point discrimination distances in the normal hand and forearm: Application to various methods of fingertip reconstruction. *Plast. Reconstr. Surg.* **59**, 59–63 (1977).
15. L. A. Jones, H. N. Ho, Warm or cool, large or small? The challenge of thermal displays. *IEEE Trans. Haptics* **1**, 53–70 (2008).
16. R. S. Johansson, I. Birznieks, First spikes in ensembles of human tactile afferents code complex spatial fingertip events. *Nat. Neurosci.* **7**, 170–177 (2004).
17. J. H. Killebrew, S. J. Bensmaïa, J. F. Dammann, P. Denchev, S. S. Hsiao, J. C. Craig, K. O. Johnson, A dense array stimulator to generate arbitrary spatio-temporal tactile stimuli. *J. Neurosci. Methods* **161**, 62–74 (2007).
18. C. H. King, M. O. Culjat, M. L. Franco, J. W. Bisley, E. Dutson, W. S. Grundfest, Optimization of a pneumatic balloon tactile display for robot-assisted surgery based on human perception. *IEEE Trans. Biomed. Eng.* **55**, 2593–2600 (2008).
19. H. Z. Tan, C. M. Reed, Y. Jiao, Z. D. Perez, E. C. Wilson, J. Jung, J. S. Martinez, F. M. Severgnini, Acquisition of 500 english words through a tactile phonemic sleeve (TAPS). *IEEE Trans. Haptics* **13**, 745–760 (2020).
20. X. Yu, Z. Xie, Y. Yu, J. Lee, A. Vazquez-Guardado, H. Luan, J. Ruban, X. Ning, A. Akhtar, D. Li, B. Ji, Y. Liu, R. Sun, J. Cao, Q. Huo, Y. Zhong, C. M. Lee, S. Y. Kim, P. Gutruf, C. Zhang, Y. Xue, Q. Guo, A. Chempakasseril, P. Tian, W. Lu, J. Y. Jeong, Y. J. Yu, J. Cornman, C. S. Tan, B. H. Kim, K. H. Lee, X. Feng, Y. Huang, J. A. Rogers, Skin-integrated wireless haptic interfaces for virtual and augmented reality. *Nature* **575**, 473–479 (2019).
21. P. J. Berkelman, R. L. Hollis, Lorentz magnetic levitation for haptic interaction: Device design, performance, and integration with physical simulations. *Int. J. Rob. Res.* **19**, 644–667 (2000).
22. A. Withana, D. Groeger, J. Steimle, Tacttoo: A thin and feel-through tattoo for on-skin tactile output, in *Proceedings of the 31st Annual ACM Symposium on User Interface Software and Technology (UIST 2018)* (ACM, 2018), pp. 365–378.
23. H. Kajimoto, Electrotactile display with real-time impedance feedback using pulse width modulation. *IEEE Trans. Haptics* **5**, 184–188 (2012).
24. D. Wang, Y. Guo, S. Liu, Y. Zhang, W. Xu, J. Xiao, Haptic display for virtual reality: Progress and challenges. *Virtual Real. Intell. Hardw.* **1**, 136–162 (2019).
25. A. Handler, D. D. Ginty, The mechanosensory neurons of touch and their mechanisms of activation. *Nat. Rev. Neurosci.* **22**, 521–537 (2021).
26. S. Maksimovic, M. Nakatani, Y. Baba, A. M. Nelson, K. L. Marshall, S. A. Wellnitz, P. Firozi, S. H. Woo, S. Ranade, A. Patapoutian, E. A. Lumpkin, Epidermal Merkel cells are mechanosensory cells that tune mammalian touch receptors. *Nature* **509**, 617–621 (2014).
27. M. Moroni, M. R. Servin-Vences, R. Fleischer, O. Sánchez-Carranza, G. R. Lewin, Voltage gating of mechanosensitive PIEZO channels. *Nat. Commun.* **9**, 1096 (2018).
28. D. R. McNeal, Analysis of a model for excitation of myelinated nerve. *IEEE Trans. Biomed. Eng.* **BME-23**, 329–337 (1976).
29. A. Akhtar, J. Sombeck, B. Boyce, T. Bretl, Controlling sensation intensity for electrotactile stimulation in human-machine interfaces. *Sci. Robot.* **3**, eaap9770 (2018).
30. R. S. Johansson, J. R. Flanagan, Coding and use of tactile signals from the fingertips in object manipulation tasks. *Nat. Rev. Neurosci.* **10**, 345–359 (2009).
31. R. Johansson, A. Vallbo, Tactile sensibility in the human hand: Relative and absolute densities of four types of mechanoreceptive units in glabrous skin. *J. Physiol.* **286**, 283–300 (1979).
32. S. J. Lederman, L. A. Jones, Tactile and haptic illusions. *IEEE Trans. Haptics* **4**, 273–294 (2011).
33. H. Kajimoto, N. Kawakami, S. Tachi, Electro-tactile display with tactile primary color approach. *Int. Conf. Intell. Robot. Syst.* **2**, 541–546 (2004).
34. U. Birgersson, E. Birgersson, S. Ollmar, Estimating electrical properties and the thickness of skin with electrical impedance spectroscopy: Mathematical analysis and measurements. *J. Electr. Bioimpedance* **3**, 51–60 (2012).
35. C. D. Mørch, K. Hennings, O. K. Andersen, Estimating nerve excitation thresholds to cutaneous electrical stimulation by finite element modeling combined with a stochastic branching nerve fiber model. *Med. Biol. Eng. Comput.* **49**, 385–395 (2011).
36. S. Gabriel, R. W. Lau, C. Gabriel, The dielectric properties of biological tissues: II. Measurements in the frequency range 10 Hz to 20 GHz. *Phys. Med. Biol.* **41**, 2251–2269 (1996).
37. S. Ye, K. Zhu, P. Li, X. Sui, Neural firing mechanism underlying two-electrode discrimination by 3D transcutaneous electrical nerve stimulation computational model. *J. Shanghai Jiaotong Univ.* **24**, 716–722 (2019).
38. K. Sato, S. Tachi, Design of electrotactile stimulation to represent distribution of force vectors, in *Proceedings of the 2010 IEEE Haptics Symposium* (IEEE, 2010), pp. 121–128.
39. V. Vechev, J. Zarate, D. Lindlbauer, R. Hinchet, H. Shea, O. Hilliges, in *Proceedings of the 26th IEEE Conference on Virtual Reality and 3D User Interfaces (VR 2019)* (IEEE, 2019), pp. 312–320.
40. S. E. Root, C. W. Carpenter, L. V. Kayser, D. Rodriquez, D. M. Davies, S. Wang, S. T. M. Tan, Y. S. Meng, D. J. Lipomi, Ionotactile stimulation: Nonvolatile ionic gels for human-machine interfaces. *ACS Omega* **3**, 662–666 (2018).
41. M. Rahimi, F. Jiang, Y. Shen, Spatiotemporal identification of moving patterns on a fingertip-based electro-tactile display array. *TechRxiv*, 1–10 (2020).
42. C. J. Poletto, C. L. Van Doren, A high voltage, constant current stimulator for electrocutaneous stimulation through small electrodes. *IEEE Trans. Biomed. Eng.* **46**, 929–936 (1999).
43. R. L. Klatzky, S. J. Lederman, in *Multisensory Object Perception in the Primate Brain* (Springer, 2010), pp. 211–230.
44. L. Wei, H. Zhou, S. Nahavandi, D. Wang, Toward a future with human hands-like haptics: A universal framework for interfacing existing and future multipoint haptic devices. *IEEE Syst. Man Cybern. Mag.* **2**, 14–25 (2016).
45. National Federation of the Blind, The braille literacy crisis in America: Facing the truth, reversing the trend, empowering the blind. *Braille Monit.* (2009).
46. N. Kitagawa, Y. Igarashi, M. Kashino, The tactile continuity illusion. *J. Exp. Psychol. Hum. Percept. Perform.* **35**, 1784–1790 (2009).
47. M. Tezuka, K. Ishimaru, N. Miki, Electrotactile display composed of two-dimensionally and densely distributed microneedle electrodes. *Sens. Actuat. A Phys.* **258**, 32–38 (2017).
48. V. Yem, H. Kajimoto, Comparative evaluation of tactile sensation by electrical and mechanical stimulation. *IEEE Trans. Haptics* **10**, 130–134 (2017).

49. L. Shu, X. Tao, D. D. Feng, A new approach for readout of resistive sensor arrays for wearable electronic applications. *IEEE Sens. J.* **15**, 442–452 (2015).

Acknowledgments
Funding: The work described here was supported by the Tencent Robotics X Laboratory and the General Research Grant (project no. CityU 11212021) and the Early Career Scheme (project no. CityU 21210619) from the Research Grants Council of the Hong Kong Special Administrative Region. **Author contributions:** Conceptualization: W.L., L.W., and Z.Y. Hardware fabrication: D.Z. and R.Z. Software and code: L.W., X.L., and G.P. Circuit board: W.W.L. and R.Z. FEA: W.L., Q.P., and Y.H. Supervision: L.W. and Z.Y. Writing: W.L., W.W.L., Y.H., H.Z.T., Z.Z., L.W., and Z.Y. **Competing interests:** The authors declare that they have no competing interests. **Data and materials availability:** All data needed to evaluate the conclusions in the paper are present in the paper and/or the Supplementary Materials. Additional data are stored at Zenodo (https://doi.org/10.5281/zenodo.6601149).

Submitted 6 March 2022
Accepted 22 July 2022
Published 9 September 2022
10.1126/sciadv.abp8738